

# SmoothOut: Smoothing Out Sharp Minima for Generalization in Large-Batch Deep Learning

**Wei Wen**  
Duke University  
wei.wen@duke.edu

**Yandan Wang**  
University of Pittsburgh  
yaw46@pitt.edu

**Feng Yan**  
University of Nevada, Reno  
fyan@unr.edu

**Cong Xu**  
Hewlett Packard Labs  
cong.xu@hpe.com

**Yiran Chen**  
Duke University  
yiran.chen@duke.edu

**Hai Li**  
Duke University  
hai.li@duke.edu

## Abstract

In distributed deep learning, a large batch size in *Stochastic Gradient Descent* is required to fully exploit the computing power in distributed systems. However, generalization gap (accuracy loss) was observed because large-batch training converges to sharp minima which have bad generalization [1][2]. This contradiction hinders the scalability of distributed deep learning. We propose *SmoothOut* to smooth out sharp minima in *Deep Neural Networks* (DNNs) and thereby close generalization gap. *SmoothOut* perturbs multiple copies of the DNN in the *parameter space* and averages these copies. We prove that *SmoothOut* can eliminate sharp minima. Perturbing and training multiple DNN copies is inefficient, we propose a stochastic version of *SmoothOut* which only introduces overhead of noise injection and denoising per iteration. We prove that the *Stochastic SmoothOut* is an unbiased approximation of the original *SmoothOut*. In experiments on a variety of DNNs and datasets, *SmoothOut* consistently closes generalization gap in large-batch training within *the same epochs*. Moreover, *SmoothOut* can guide small-batch training to flatter minima and improve generalization.

## 1 Introduction

Training *Deep Neural Networks* (DNNs) is time-consuming. *Stochastic Gradient Descent* (SGD) is the dominant optimization method used for DNN training for its computation efficiency. However, SGD can still be slow as DNN size grows and data explodes, especially in large-scale industrial applications [3][4]. It is natural to incorporate more computing resources and increase parallelism for accelerating SGD. An effective solution is *Distributed Deep Learning*, which leverages high parallelism in distributed systems [5][6][7]. Typically, in data parallelism, the mini-batch size of SGD is  $N \cdot B$ , where  $B$  is the batch size of training samples fed into each worker<sup>1</sup> and  $N$  is the number of workers.  $B$  is usually a constant but large enough to fully exploit computing and memory capacity in each worker while  $N$  keeps increasing, therefore, in large-scale distributed deep learning, the mini-batch size is very large. This is referred to as *large-batch deep learning*.

However, accuracy loss has been widely observed in large-batch deep learning [2][7][8]. The accuracy difference between small-batch training and large-batch training is the well known “generalization gap” [2]. Reasons behind this observation are still under active research. Hoffer *et al.* [9] hypothesizes that the process of SGD is similar to “random walk on a random potential” [10]. This hypothesis

<sup>1</sup>A worker is a computing node, which can be a CPU, a GPU, an FPGA and any hardware computing unit.

attributes generalization gap to the limited number of parameter updates, and suggests to train more iterations. *Learning rate tuning* was also proposed to match walk statistics to close the gap.

Inspired by Hoffer *et al.* [9], a series of practical techniques are proposed [7][11][12][13]. Another appealing hypothesis, which arouses recent research interest, is that large-batch SGD converges to sharp minima [2] which have bad generalization due to their high over-fitting to training data [1][14] and high sensitivity to noises [15]. Recently, Jastrzebski *et al.* [16] showed the connection between these two hypotheses: learning rate tuning motivated by “random walk” leads to flatter minima and helps to close generalization gap. Our approach is motivated by the second hypothesis, targeting on escaping sharp minima for better generalization. Moreover, our approach can enhance techniques inspired by the first hypothesis and further improve generalizability.

Keskar *et al.* [2] attempted to escape sharp minima through data augmentation, conservative training and adversarial training. However, all trials “do not completely remedy the problem” [2], leaving how to avoid sharp minima as an open question. We propose *SmoothOut* to smooth out sharp minima and guide the convergence of large-batch SGD to flatter regions. *SmoothOut* slightly perturbs DNN *function* in parameter space by injecting random noise and then averages all perturbed DNNs. Because sharp minima are sensitive to noise, slight perturbation can result in significant function increase at each sharp minimum, which means the averaged value will be high. In this way, sharp minima can be eliminated. Conversely, small perturbation only influences the margin of each flat region and the “flat bottom” still aligns well with the original “bottom”. Averaging aligned “bottoms” can maintain the original minimum. Beyond this intuition, we prove that *SmoothOut* under uniform noises can eliminate sharp minima while maintaining flat minima. However, training and averaging over many perturbed DNNs is computation intensive. We propose a stochastic version of *SmoothOut*, named as *Stochastic SmoothOut*, which injects noise per iteration during SGD. We prove that *Stochastic SmoothOut* is equivalent to the original *SmoothOut* in expectation. Our experiments show that *SmoothOut* can help to escape sharp minima and close the generalization gap within the same epochs *without* training longer as adopted by Hoffer *et al.* [9]. *SmoothOut* is easy to be implemented and our source code is publicly available at <https://github.com/wenwei202/smoothout>.

## 2 Related work

Why deep neural networks generalize well still needs deeper understanding [17]. One hypothesis is that SGD finds flat minima which can generalize well [1][2]. As Hochreiter *et al.* [1] pointed out, based on Minimum Description (Message) Length [14][18] theory, a flatter minimum can be encoded in fewer bits which indicates simpler DNN model for better generalization. Alternative explanations are based on Bayesian learning [19][20]. Dinh *et al.* [21] further argue that current definitions of sharpness are problematic and redefinition is required for explanation. Typically, for DNNs with rectifier non-linearity, the sharpness can be easily manipulated through reparametrization [21]. However, Keskar *et al.* [2] found that large-batch training has bad generalization because it indeed sticks to sharp minima. Different from previous work, we focus on new variants of SGD to escape sharp minima. We find that our method not only can escape sharp minima during large-batch training but also guide small-batch training to converge to flatter ones, therefore, improving generalization in both cases. A related work by Chaudhari *et al.* [15] proposed Entropy-SGD which maximizes local entropy to bias SGD to flat minima (“wide valleys”). Local entropy was constructed by building connections between Gibbs distribution and optimization problems. The gradients of local entropy was estimated by Langevin dynamics [22], which is computation intensive. Compared with Entropy-SGD, our *SmoothOut* is more efficient since noise injection and denoising is the only overhead. This enables *SmoothOut* to scale to larger dataset like ImageNet [23]. Moreover, *SmoothOut* consistently improves generalization in all experiments, while Entropy-SGD achieved “comparable generalization error”.

In this work, we focus on escaping sharp minima in large-batch SGD to facilitate distributed deep learning. As aforementioned, Hoffer *et al.* [9] suggest to train more epochs to close generalization gap, however, training more epochs consumes more time. Whether large-batch training can generalize well without extending epochs remains open. To answer this question, heuristic techniques were proposed to close the gap without prolonging epochs. Those techniques include linearly learning rate scaling [7][24], warm-up training [7][13] and Layer-wise Adaptive Rate Scaling [12]. However, without theoretical support, it is unclear to what extent those methods can generalize. For example, linear learning rate scaling and warm-up training proposed in [7] cannot generalize to CIFAR-

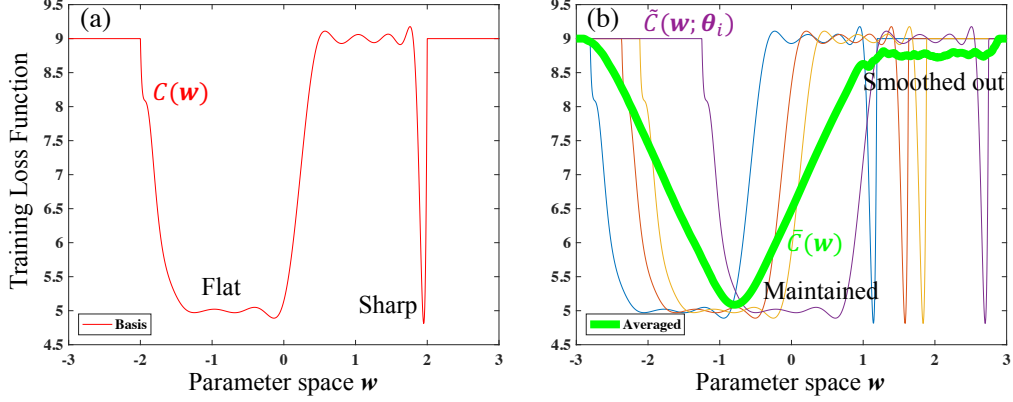


Figure 1: A simple example to illustrate the basic idea of *SmoothOut*. (a) The training loss function of the basis model w.r.t. parameter  $w$ . (b) Each thin curve represents a perturbed model; there are totally 1024 perturbations, but only four are plotted for cleaner visualization; the perturbation is done by slightly shifting the basis model in (a); the shift distance is randomly drawn from a uniform distribution; the green curve is a new model by averaging over all perturbations.

10 [9] and other architectures on ImageNet [12]. Compared with those techniques, our *SmoothOut* is an interpretable solution supported by the “sharp minima” hypothesis. *SmoothOut* can close generalization gap within the same epochs for various DNNs on various datasets.

### 3 SmoothOut: Principles, Theory and Implementation

We first introduce our *SmoothOut* method and its principles in Section 3.1. To reduce computation complexity, *Stochastic SmoothOut* is proposed in Section 3.2; we prove that *Stochastic SmoothOut* is an unbiased approximation of deterministic *SmoothOut*. Section 3.3 implements *Stochastic SmoothOut* in back-propagation of DNNs.

#### 3.1 Principles: Averaging Perturbed Models Smooths Out Sharp Minima

As Keskar *et al.* [2] studied, sharp minima have large generalization gaps, because small distortion/shift of testing function from training function can significantly increase testing loss even though current parameter is a minimum of the training function<sup>2</sup>. Our optimization goal is to encourage convergence to flat minima for more robust models. Our solution is derived from the sensitivity nature of sharp minima. We intentionally inject noises into the *model* to smooth out sharp minima. The concept is illustrated in Figure 1. We define  $w$  as a point in the parameter space,  $C(w)$  as the training loss function and  $\tilde{C}(w; \Theta)$  as a perturbation of  $C(w)$ .  $\tilde{C}(w; \Theta)$  is parameterized by both  $w$  and  $\Theta$ , where  $\Theta$  is a random vector to generate the perturbation. Instead of minimizing  $C(w)$ , we propose to minimize

$$\bar{C}(w) = \mathbf{E} \left\{ \tilde{C}(w; \Theta) \right\} \approx \frac{1}{N} \sum_{i=1}^N \tilde{C}(w; \theta_i) \quad (1)$$

to find a optimal  $w^*$  for  $C(w)$ , where  $\theta_i$  is a sample of  $\Theta$  and  $N$  is the number of samples. For simplicity, we assume  $C(w)$  has one flat minimum  $w_f$  and one sharp minimum  $w_s$ , but the discussion can be generalized to  $C(w)$  with multiple flat and sharp minima. Our goal is to design an auxiliary function  $\bar{C}(w)$  such that its minimum within the original flat region can approximate  $w_f$ , by satisfying the *Flat Constraint*

$$\left| \arg \min_{w \in \mathcal{D}(w_f, \tau)} (\bar{C}(w)) - w_f \right| \leq \varphi, \quad (2)$$

meanwhile the sharp  $w_s$  is smoothed out, by satisfying the *Sharp Constraint*

$$\min_{\mathcal{D}(w_s, \varepsilon)} (\bar{C}(w)) \geq \max_{\mathcal{D}(w_s, \varepsilon)} (C(w)) > \min_{\mathcal{D}(w_f, \tau)} (\bar{C}(w)), \quad (3)$$

<sup>2</sup>Figure 1 in their paper [2] illustrates this conception.

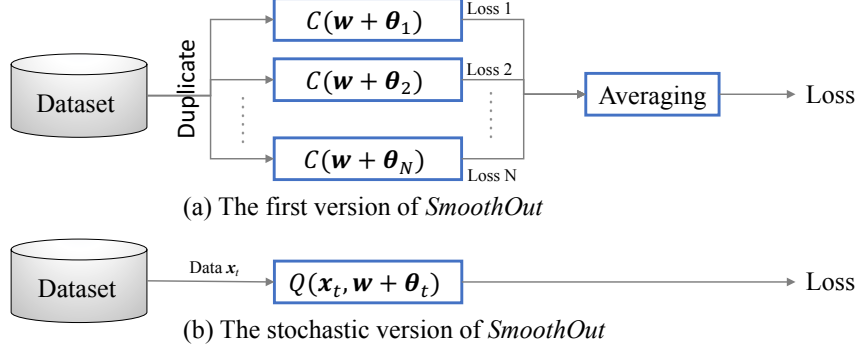


Figure 2: The framework of *SmoothOut* under *Uniform Perturbation*: (a) the first version of proposed *SmoothOut* in Eq. (1); (b) the *Stochastic SmoothOut* which randomly perturbs parameter  $\mathbf{w}$  at each batch. *Stochastic SmoothOut* will be introduced in Section 3.2.

where  $\mathcal{D}(\mathbf{w}, \varsigma)$  represents a region around  $\mathbf{w}$ , being constrained as

$$\mathcal{D}(\mathbf{w}, \varsigma) = \{\mathbf{w}' \in \mathbb{R}^m : |(\mathbf{w}' - \mathbf{w})_i| \leq \varsigma, \forall i \in \{1, 2, \dots, m\}\}. \quad (4)$$

When  $\varphi$  is small and  $\tau$  is large, Inequality (2) ensures that the auxiliary function  $\bar{C}(\mathbf{w})$  maintains the minimality of  $C(\mathbf{w})$  in the flat region; in the extreme case of  $\varphi = 0$  and  $\tau \rightarrow \infty$ , the minimum of  $\bar{C}(\mathbf{w})$  is exactly  $\mathbf{w}_f$ . Conversely, near the original sharp region, Inequality (3) ensures that minimality of  $\bar{C}(\mathbf{w})$  is eliminated when  $\varepsilon$  is relatively large, because  $\max_{\mathcal{D}(\mathbf{w}_s, \varepsilon)} (C(\mathbf{w}))$ , the lower bound of  $\bar{C}(\mathbf{w})$ , increases rapidly by slightly increasing  $\varepsilon$  around the sharp minimum; in the extreme case of  $\varepsilon \rightarrow \infty$ , the lower bound is the maximum of  $C(\mathbf{w})$ . In a nutshell, a good design of  $\bar{C}(\mathbf{w})$  allow a small  $\varphi$ , a large  $\tau$  and a large  $\varepsilon$ . In this way, minimization process of  $\bar{C}(\mathbf{w})$  will skip  $\mathbf{w}_s$  and converge to  $\mathbf{w}_f$ . It is infeasible to find an optimal  $\bar{C}(\mathbf{w})$  which minimizes  $\varphi$  and maximizes  $\tau$  and  $\varepsilon$ , especially when  $C(\mathbf{w})$  is a deep neural network. However, we find that, under the *Uniform Perturbation*

$$\tilde{C}(\mathbf{w}; \Theta) = C(\mathbf{w} + \Theta) \text{ where } \Theta_i \stackrel{\text{i.i.d.}}{\sim} U(-a, a) \text{ and } \forall i \in \{1, 2, \dots, m\}, \quad (5)$$

$\tilde{C}(\mathbf{w})$  can well perform the purpose.  $U(-a, a)$  is a uniform distribution within a range of  $[-a, a]$ <sup>3</sup>. In the Appendix A, we prove that, under *Uniform Perturbation*, appropriate  $\varphi$ ,  $\tau$  and  $\varepsilon$  can be found to satisfy *Flat Constraint* and *Sharp Constraint*:

**Theorem 1.** When  $C(\mathbf{w})$  is symmetric in  $\mathcal{D}(\mathbf{w}_f, \tau)|_{\tau > a}$ , the minimum of  $\varphi$  is 0 to satisfy the *Flat Constraint* when  $\tilde{C}(\mathbf{w})$  is generated under the *Uniform Perturbation*.

**Theorem 2.** Suppose  $C(\mathbf{w})$  is high dimensional ( $\mathbf{w} \in \mathbb{R}^m, m \rightarrow \infty$ ) and is symmetric and strictly monotonic in  $\mathcal{D}(\mathbf{w}_s, b)|_{b > a}$ , then  $\exists a$  such that *Sharp Constraint* is satisfied with  $\varepsilon \rightarrow a^-$  when  $\tilde{C}(\mathbf{w})$  is generated under the *Uniform Perturbation*.

Besides the rigor proof in the Appendix A, *SmoothOut* can be explained from the perspective of signal processing: imagining the parameter space as a time domain and the function as signals, then averaging is a low-pass filter which eliminates high-frequency signals (sharp regions) while maintains low-frequency signals (flat regions).

Figure 2(a) illustrates the framework of the proposed *SmoothOut* in SGD. All models share the same parameter  $\mathbf{w}$ . Before training starts, the  $i$ -th model is independently perturbed by  $\theta_i$ ; during training, all  $\theta_i$  are fixed and an identical batch of data is sent to all models for training. Because a large  $N$  is required for approximation in Eq. (1), the computation complexity and memory usage will be very high, especially when  $C(\mathbf{w})$  is a deep neural network. In Section 3.2, the *Stochastic SmoothOut* will be proposed to solve this issue.

### 3.2 Theory: *Stochastic SmoothOut* is Unbiased

To reduce the computation complexity and memory usage of *SmoothOut* in Figure 2(a), *Stochastic SmoothOut* is proposed in this section as shown in Figure 2(b). Instead of using multiple perturbed

<sup>3</sup>In this case, we have abused  $\tilde{C}(\mathbf{w}; a)$  as  $\tilde{C}(\mathbf{w})$  in the notation for simplicity.

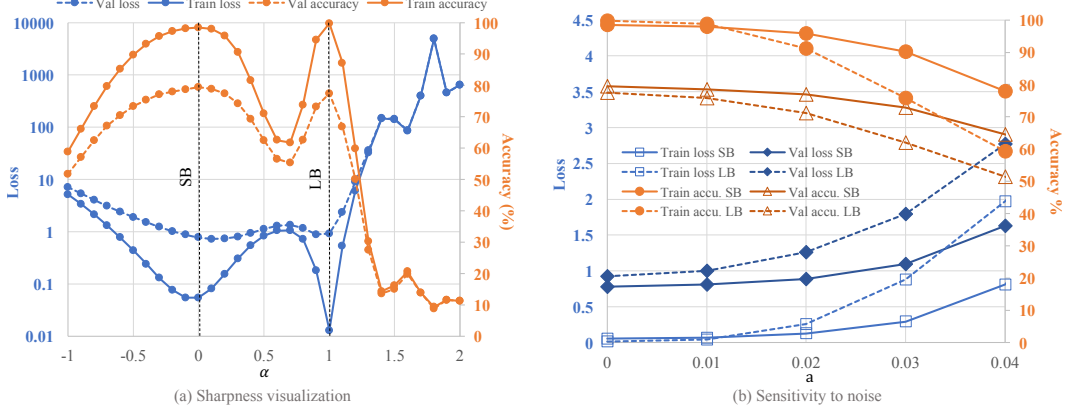


Figure 3: Notation: “SB”: Small Batch (256); “LB”: Large Batch (5000); “accu.”: accuracy. (a) loss and accuracy vs.  $\alpha$ , which controls  $\mathbf{w}$  along the direction from SB minimum ( $\mathbf{w}_f$ ) to LB minimum ( $\mathbf{w}_s$ ); (b) loss and accuracy under influence of different strengths of noise. Dataset: CIFAR-10. Network:  $C_1$  in [2] implemented by [9]. Optimizer: Adam with 0.001 initial learning rate.

models to learn from identical data, only one model is trained. At the  $t$ -th batch of training data  $\mathbf{x}_t$ , the parameter  $\mathbf{w}_t$  is first perturbed to  $\mathbf{w}_t + \boldsymbol{\theta}_t$  and then  $\mathbf{x}_t$  is fed into the model to calculate the loss function. We can prove that, in both frameworks, the outputs can approximate  $\bar{C}(\mathbf{w})$  without bias.

Formally, in Figure 2(a), the expectation of the output is

$$\mathbf{E}_{\boldsymbol{\theta}_{1 \dots N}} \left\{ \frac{1}{N} \sum_{i=1}^N C(\mathbf{w} + \boldsymbol{\theta}_i) \right\} = \mathbf{E}_{\boldsymbol{\Theta}} \{C(\mathbf{w} + \boldsymbol{\Theta})\} = \bar{C}(\mathbf{w}). \quad (6)$$

In online learning systems [25] like Figure 2(b), the data  $\mathbf{x}_t$  is independently generated from a random distribution and its online loss is obtained by model  $Q(\mathbf{x}_t, \mathbf{w})$ ; the final loss function to minimize is the expectation of online loss under data distribution, *i.e.*,

$$C(\mathbf{w}) \triangleq \mathbf{E}_{\mathbf{X}} \{Q(\mathbf{x}, \mathbf{w})\}. \quad (7)$$

Therefore, in Figure 2(b), the expectation of the output is

$$\mathbf{E} \{Q(\mathbf{x}_t, \mathbf{w} + \boldsymbol{\theta}_t)\} = \mathbf{E}_{\boldsymbol{\Theta}} \{\mathbf{E}_{\mathbf{X}} \{Q(\mathbf{x}, \mathbf{w} + \boldsymbol{\Theta})\}\} = \mathbf{E}_{\boldsymbol{\Theta}} \{C(\mathbf{w} + \boldsymbol{\Theta})\} = \bar{C}(\mathbf{w}). \quad (8)$$

Consequently, both frameworks in Figure 2 can approximate  $\bar{C}(\mathbf{w}) = \mathbf{E}\{\tilde{C}(\mathbf{w}; \boldsymbol{\Theta})\}$  in Eq. (1), but *Stochastic SmoothOut* is much more computation efficient. The only overhead of *Stochastic SmoothOut* is noise injection and denoising as will be shown in Section 3.3. In the following sections, without explicit clarification, *SmoothOut* will refer to the stochastic version in Figure 2(b).

As indicated in the proof of *Sharp Constraint*, the reason why *SmoothOut* can eliminate sharp minima is that  $C(\mathbf{w}_s)$  is more sensitive to noise than  $C(\mathbf{w}_f)$ , and we expect  $\bar{C}(\mathbf{w}_s)$  increases faster than  $\bar{C}(\mathbf{w}_f)$  as  $a$  increases from 0. To verify this, we first train a DNN under a small batch size to get a flat minimum  $\mathbf{w}_f$ ; second,  $\mathbf{w} = \mathbf{w}_f$  is deployed into the framework in Figure 2(b); third, the whole train/validation dataset is fed to the framework in batch size of 100, and at each batch, the parameter is perturbed to  $\mathbf{w} = \mathbf{w}_f + \boldsymbol{\theta}_t$ ; finally, the losses are averaged over all batches to estimate  $\bar{C}(\mathbf{w}_f)$ . The same process is done using a large batch size for the same DNN to estimate  $\bar{C}(\mathbf{w}_s)$ . We scan  $a$  in a range to test the sensitivity of  $\bar{C}(\mathbf{w}_f)$  and  $\bar{C}(\mathbf{w}_s)$  to perturbation. Figure 3(a) visualizes the sharpness of  $C(\mathbf{w})$  around  $\mathbf{w}_f$  and  $\mathbf{w}_s$ , using the technique adopted in [2] which was originally proposed in [26]. In Figure 3(a), each point on the loss curve is  $(\mathbf{w}^+, C(\mathbf{w}^+))$  where  $\mathbf{w}^+ = \alpha \cdot \mathbf{w}_s + (1 - \alpha) \cdot \mathbf{w}_f$ . The visualization is consistent with [2], which concluded that large-batch training converges to sharp minima. Figure 3(b) analyzes the sensitivity. For both training and validation datasets,  $\bar{C}(\mathbf{w}_s)$  indeed increases faster than  $\bar{C}(\mathbf{w}_f)$  as  $a$  increases. The accuracy curves have a similar trend. Sensitivity analyses of more DNNs and more datasets are included in the Appendix B. Therefore, a side outcome of this work is that we can use

$$s = \frac{\Delta(\bar{C}(\mathbf{w}^*; a))}{\Delta a} \quad (9)$$

as a metric to measure the sharpness of  $C(\mathbf{w})$  at minimum  $\mathbf{w}^*$ . A larger  $s$  means a sharper minimum.

### 3.3 Implementation: Back-propagation with Perturbation and Denoising

In Figure 2(b), the gradient to update parameter at iteration  $t$  is

$$\mathbf{g}_t = \left. \frac{\partial Q(\mathbf{x}_t, \mathbf{w} + \boldsymbol{\theta}_t)}{\partial \mathbf{w}} \right|_{\mathbf{w}=\mathbf{w}_t} = \nabla_{\mathbf{w}} Q(\mathbf{x}_t, \mathbf{w})|_{\mathbf{w}=\mathbf{w}_t + \boldsymbol{\theta}_t} \cdot \frac{\partial(\mathbf{w} + \boldsymbol{\theta}_t)}{\partial \mathbf{w}}. \quad (10)$$

Therefore, the parameter is updated as

$$\mathbf{w}_{t+1} = \mathbf{w}_t - \eta_t \cdot \nabla_{\mathbf{w}} Q(\mathbf{x}_t, \mathbf{w})|_{\mathbf{w}=\mathbf{w}_t + \boldsymbol{\theta}_t}, \quad (11)$$

where  $\eta_t$  is the learning rate and the gradient is obtained by back propagation when the parameter value is  $\mathbf{w}_t + \boldsymbol{\theta}_t$ . Thus, *SmoothOut* can be implemented as Algorithm 1 as illustrated in Figure 4. This reveals a pitfall in implementation that the noise  $\boldsymbol{\theta}_t$  added to  $\mathbf{w}_t$  must be denoised before applying the gradient.

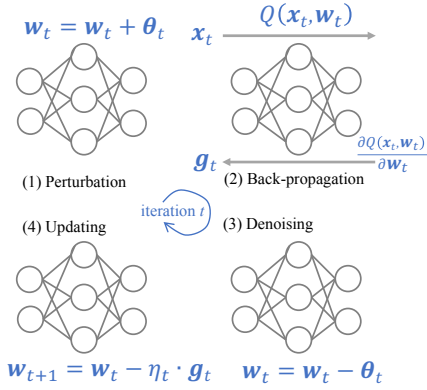


Figure 4: *SmoothOut* in BP.

#### Algorithm 1 *SmoothOut* in Back Propagation

**Input** : Training dataset  $\mathbf{X}$ , total iterations  $T$ , model  $Q(\mathbf{x}, \mathbf{w})$  with initial parameter  $\mathbf{w} = \mathbf{w}_0$

- 1: **for**  $t \in \{0, \dots, T-1\}$  **do**
- 2: Randomly sample a batch data  $\mathbf{x}_t$  from  $\mathbf{X}$
- 3: Perturbation:  $\mathbf{w}_t = \mathbf{w}_t + \boldsymbol{\theta}_t$  where  $\boldsymbol{\theta}_{ti} \stackrel{\text{i.i.d.}}{\sim} U(-a, a)$
- 4: Back-propagation:  $\mathbf{g}_t = \frac{\partial Q(\mathbf{x}_t, \mathbf{w}_t)}{\partial \mathbf{w}_t}$
- 5: Denoising:  $\mathbf{w}_t = \mathbf{w}_t - \boldsymbol{\theta}_t$
- 6: Updating:  $\mathbf{w}_{t+1} = \mathbf{w}_t - \eta_t \cdot \mathbf{g}_t$
- 7: **end for**

**Output** :

- 1 The model  $Q(\mathbf{x}, \mathbf{w})$  with final parameter  $\mathbf{w} = \mathbf{w}_T$

As shown in Algorithm 1, the only overhead of *SmoothOut* is adding and subtracting noises, which is much more efficient than training multiple DNNs in Figure 2(a). Note that, although Algorithm 1 is proposed in the context of vanilla SGD, it can be extended to SGD variants by simply utilizing the gradient  $\mathbf{g}_t$  for momentum accumulation, learning rate adaptation, and so on.

## 4 Experiments

We evaluate *SmoothOut* in MNIST [27], CIFAR-10 [28], CIFAR-100 [28] and ImageNet [23] dataset. DNNs and training methods used in Hoffer *et al.* [9] and Keskar *et al.* [2] are selected as the baselines. In large-batch training of models of Hoffer *et al.* [9], “learning rate tuning” and *Ghost Batch Normalization* (GBN) proposed by the authors are used; however, we do not adopt “regime adaptation” because it increases epochs linearly w.r.t. batch size and therefore linearly increases training time. In our experiments, large-batch (“LB”) training stops in the same epochs of small-batch (“SB”) training. In each training, the best validation top-1 accuracy is reported.  $(\mathcal{C}_\epsilon, A)$ -sharpness [2] is utilized to measure the sharpness of a minimum, which is solved using L-BFGS-B algorithm [29]. In solving  $(\mathcal{C}_\epsilon, A)$ -sharpness, the full-space (*i.e.*,  $A = I_n$ ) in the bounding box  $\mathcal{C}_\epsilon$  (with  $\epsilon = 5 \cdot 10^{-4}$ ) is explored to find the maximum for measurement. As L-BFGS-B is an estimation algorithm and may fail to find the exact maximum value, variance in measurements is observed. We run 5 experiments for each measurement, and use the *maximum* as the final sharpness metric. Unlike Keskar *et al.* [2] which *averaged* over 5 runs, ours is more reasonable because  $(\mathcal{C}_\epsilon, A)$ -sharpness is based on measuring the maximum value around the box.

Table 1 summarizes DNNs and their training methods in the baselines. All baseline models are duplicated using the source code of Hoffer *et al.* [9]<sup>4</sup>. In the table, large-batch training always has sharper minima and lower accuracy. Consistent with conclusions by Jastrzebski *et al.* [16], “learning rate tuning” by Hoffer *et al.* [9] indeed can reduce the sharpness, however, it can not fully close the gap when training epochs are not prolonged (*i.e.*, without using “regime adaptation”).

<sup>4</sup><https://github.com/eladhoffer/bigBatch>

Table 1: Baseline models.

DNN	Dataset	Data augment	Optimizer	Epochs	Learning rate	GBN	Batch size	Accuracy	$(C_e, A)$ -sharpness
$F_1$ (Keskar <i>et al.</i> [2]) <sup>†</sup>	MNIST	No	Adam	200	0.001	No	256 6000	98.49% 98.01%	0.0000 57.8246
$C_1$ (Keskar <i>et al.</i> [2]) <sup>†</sup>	CIFAR-10	No	Adam	200	0.001	No	256 5000	79.67% 77.30%	27.7448 117.8266
$C_3$ (Keskar <i>et al.</i> [2]) <sup>†</sup>	CIFAR-100	No	Adam	200	0.001	No	256 5000	47.99% 44.37%	23.5103 62.0682
<i>ResNet44</i> (He <i>et al.</i> [30])	CIFAR-10	Yes	Momentum	200	0.1	No	128	93.18%	132.3693
<i>ResNet44</i> (He <i>et al.</i> [30])					0.1	No	2048	87.58%	459.1477
<i>ResNet44</i> (Hoffer <i>et al.</i> [9]) <sup>†</sup>					0.4	Yes	2048	89.24%	252.0197
<i>ResNet44</i> (He <i>et al.</i> [30])	CIFAR-100	Yes	Momentum	200	0.1	No	128	70.26%	0.0000
<i>ResNet44</i> (He <i>et al.</i> [30])					0.1	No	1024	64.67%	203.7407
<i>ResNet44</i> (Hoffer <i>et al.</i> [9]) <sup>†</sup>					0.283	Yes	1024	67.23%	140.4747
<i>AlexNet</i> (Krizhevsky <i>et al.</i> [31])	ImageNet	Yes	Momentum	60	0.01	No	256	56.15%	595.9811
<i>AlexNet</i> (Hoffer <i>et al.</i> [9]) <sup>†</sup>					0.113	Yes	16384	47.64%	623.0147

<sup>†</sup> Models that are targeted on to close generalization gap by *SmoothOut*.

Table 2: *SmoothOut* in both small-batch training and large-batch training.

DNN	Dataset	Batch size	Baseline	<i>SmoothOut</i>	Improvement	$(C_e, A)$ -sharpness change baseline $\rightarrow$ <i>SmoothOut</i>
$F_1$ (Keskar <i>et al.</i> [2])	MNIST	256	98.49%	<b>98.61%</b>	0.12%	0.0000 $\rightarrow$ <b>0.0000</b>
		6000	98.01%	<b>98.42%</b>	0.41%	57.8246 $\rightarrow$ <b>5.4128</b>
$C_1$ (Keskar <i>et al.</i> [2])	CIFAR-10	256	79.67%	<b>81.72%</b>	2.05%	27.7448 $\rightarrow$ <b>0.0003</b>
		5000	77.30%	<b>80.34%</b>	3.04%	117.8266 $\rightarrow$ <b>0.0004</b>
$C_3$ (Keskar <i>et al.</i> [2])	CIFAR-100	256	47.99%	<b>51.17%</b>	3.18%	23.5103 $\rightarrow$ <b>0.0001</b>
		5000	44.37%	<b>48.43%</b>	4.06%	62.0682 $\rightarrow$ <b>10.7303</b>

#### 4.1 Closing Generalization Gap within the Same Epochs

In training with *SmoothOut*, all hyper-parameters in the baseline are kept unchanged. The comparison with Keskar *et al.* [2] is in Table 2. Note that Keskar *et al.* [2] did not target on achieving state-of-the-art accuracy but studying the characteristics of minima, and we simply follow this purpose in Table 2. Comparison with more state-of-the-art models by Hoffer *et al.* [9] will be covered in Table 3.

In Table 2, *SmoothOut* is evaluated in both small-batch (SB) and large-batch (LB) training, and Figure 5 visualizes and compares the sharpness of baseline ( $C_3$ ) and *SmoothOut*. Similar visualization results for  $F_1$  and  $C_1$  can be found in the Appendix C. In Table 2 and Figure 5, we observed consistency among sharpness, visualization, and generalization, that is, a smaller  $(C_e, A)$ -sharpness, then a flatter region in the visualization and a higher accuracy. In summary, the result indicates that (1) comparing with SB training, LB training converges to sharper minima with worse generalization, but *SmoothOut* can converge to flatter minima and closes the gap or even improves the accuracy; (2) the sharp minima problem may also exist in SB training as shown in Figure 5(a), but *SmoothOut* can reduce the sharpness and improve the accuracy even for SB training; (3) sharp minima problem is more severe in LB training such that *SmoothOut* can improve more in LB scenario.

In Table 3, the baseline (Hoffer *et al.* [9]) is the LB training with “learning rate tuning” and GBN, which can reduce generalization gap but cannot close it within the same epochs. *SmoothOut* is simply added on top of baseline for comparison. The results show that *SmoothOut* can further reduce the sharpness and the generalization gap upon the state-of-the-art method. However, *SmoothOut* cannot fully close the gap in the deeper neural networks. It attributes to the fact that the weight distributions across all layers vary a lot, adding noise with a constant strength to all weights can over-perturb the layers with small weights. The varying distribution is also the source of problem in visualizing the sharpness as pointed out in [32]. To overcome this, [32] proposed “filter normalization” and achieved more accurate visualization. Inspired by “filter normalization”, in *SmoothOut*, the noises added to a filter are linearly scaled by the length of the filter. In fully-connected layers, the noises are scaled per neuron, *i.e.*, all input connections of each neuron form a vector and noises are scaled per vector. We call it *Adaptive SmoothOut* (*AdaSmoothOut*) because it adapts the strength of noises to the filters instead of fixing the strength. As shown in Table 3, *AdaSmoothOut* achieves better generalization than *SmoothOut* in both CIFAR-10 and CIFAR-100, especially closing the gap for

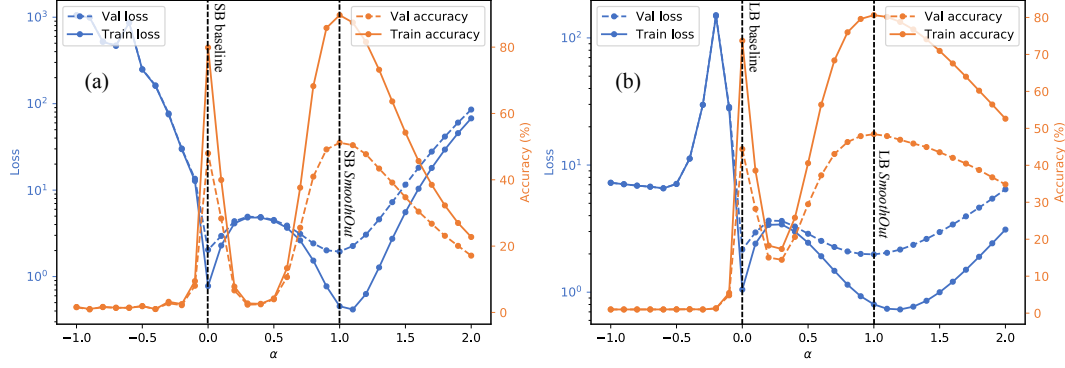


Figure 5: Sharpness of baseline and *SmoothOut* in (a) ‘SB’ training and (b) ‘LB’ training of  $C_3$ .

Table 3: *SmoothOut* and *AdaSmoothOut* improve the state-of-the-art baselines.

DNN	Dataset	Batch size	Method	Accuracy	Gap <sup>†</sup>	$(C_e, A)$ -sharpness
<i>ResNet44</i> (Hoffer <i>et al.</i> [9])	CIFAR-10	2048	Baseline	89.24%	3.94%	252.0197
			<i>SmoothOut</i>	89.83%	3.35%	204.9006
			<i>AdaSmoothOut</i>	91.20%	1.98%	348.3411
<i>ResNet44</i> (Hoffer <i>et al.</i> [9])	CIFAR-100	1024	Baseline	67.23%	3.03%	140.4747
			<i>SmoothOut</i>	68.68%	1.58%	102.9927
			<i>AdaSmoothOut</i>	70.09%	0.17%	89.0498
<i>AlexNet</i> (Hoffer <i>et al.</i> [9])	ImageNet	16384	Baseline	47.64%	8.51%	623.0147
			<i>AdaSmoothOut</i>	52.53%	3.62%	541.2508

<sup>†</sup> Generalization gap defined as small-batch accuracy minus large-batch accuracy.

*ResNet44* in CIFAR-100. As *AdaSmoothOut* is more effective in CIFAR-10 and CIFAR-100, we only evaluate *AdaSmoothOut* in ImageNet for faster development. Moreover, as *AdaSmoothOut* regularizes the trained model by averaging online, the regularizations by weight decay and dropout are not adopted in training with ImageNet, such that we can reduce the number of hyperparameters. In *AlexNet*, *AdaSmoothOut* further reduces the generalization gap by 4.89% comparing with [9].

However, under *AdaSmoothOut*, the  $(C_e, A)$ -sharpness of *ResNet44* in CIFAR-10 even increases. This exception brings us to the open question regarding appropriate definition of sharpness as broadly discussed in [21]. The authors proved that the sharpness of DNNs (with rectifier non-linearity) can be manipulated by ‘ $\alpha$ -scale transformation’ without losing generalization [21]. However, ‘filter normalization’ [32] may eliminate the impact from ‘ $\alpha$ -scale transformation’ and showed higher correlation between visualized sharpness and generalization. With ‘filter normalization’ visualization, *AdaSmoothOut* indeed converges to slightly flatter region than *SmoothOut* as visualized in Figure 6.

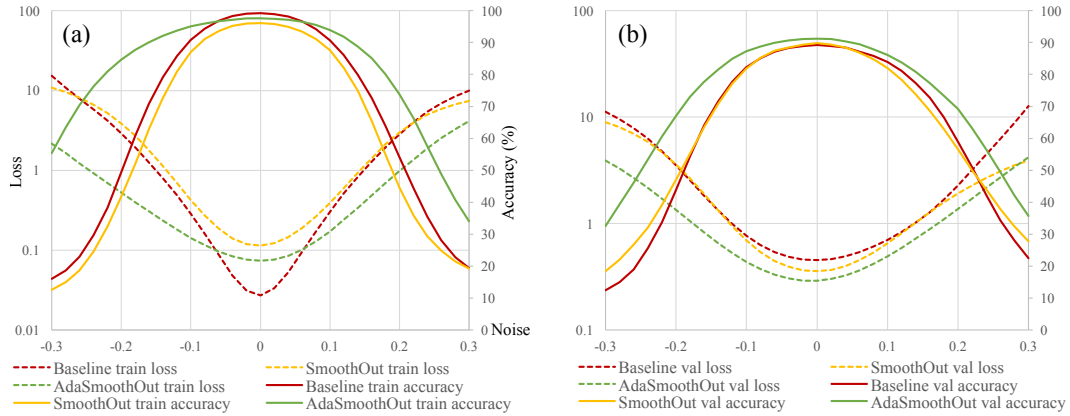


Figure 6: Sharpness visualization by ‘filter normalization’ [32] using (a) training dataset and (b) validation dataset. The DNN is *ResNet44* trained by CIFAR-10 using baseline [9], *SmoothOut* and *AdaSmoothOut*.

## References

- [1] Sepp Hochreiter and Jürgen Schmidhuber. Flat minima. *Neural Computation*, 9(1):1–42, 1997.
- [2] Nitish Shirish Keskar, Dheevatsa Mudigere, Jorge Nocedal, Mikhail Smelyanskiy, and Ping Tak Peter Tang. On large-batch training for deep learning: Generalization gap and sharp minima. In *International Conference on Learning Representations*, 2017.
- [3] Dario Amodei, Sundaram Ananthanarayanan, Rishita Anubhai, Jingliang Bai, Eric Battenberg, Carl Case, Jared Casper, Bryan Catanzaro, Qiang Cheng, Guoliang Chen, et al. Deep speech 2: End-to-end speech recognition in english and mandarin. In *International Conference on Machine Learning*, pages 173–182, 2016.
- [4] Rafal Jozefowicz, Oriol Vinyals, Mike Schuster, Noam Shazeer, and Yonghui Wu. Exploring the limits of language modeling. *arXiv preprint arXiv:1602.02410*, 2016.
- [5] Jeffrey Dean, Greg Corrado, Rajat Monga, Kai Chen, Matthieu Devin, Mark Mao, Marc'aurelio Ranzato, Andrew Senior, Paul Tucker, Ke Yang, Quoc V. Le, and Andrew Y. Ng. Large scale distributed deep networks. In *Advances in Neural Information Processing Systems*, pages 1223–1231. 2012.
- [6] Trishul M Chilimbi, Yutaka Suzue, Johnson Apacible, and Karthik Kalyanaraman. Project adam: Building an efficient and scalable deep learning training system. In *OSDI*, volume 14, pages 571–582, 2014.
- [7] Priya Goyal, Piotr Dollár, Ross Girshick, Pieter Noordhuis, Lukasz Wesolowski, Aapo Kyrola, Andrew Tulloch, Yangqing Jia, and Kaiming He. Accurate, large minibatch sgd: training imagenet in 1 hour. *arXiv preprint arXiv:1706.02677*, 2017.
- [8] Greg Diamos, Shubho Sengupta, Bryan Catanzaro, Mike Chrzanowski, Adam Coates, Erich Elsen, Jesse Engel, Awni Hannun, and Sanjeev Satheesh. Persistent rnns: Stashing recurrent weights on-chip. In *International Conference on Machine Learning*, pages 2024–2033, 2016.
- [9] Elad Hoffer, Itay Hubara, and Daniel Soudry. Train longer, generalize better: closing the generalization gap in large batch training of neural networks. In *Advances in Neural Information Processing Systems*, pages 1729–1739, 2017.
- [10] Jean-Philippe Bouchaud and Antoine Georges. Anomalous diffusion in disordered media: statistical mechanisms, models and physical applications. *Physics reports*, 195(4-5):127–293, 1990.
- [11] Samuel L Smith, Pieter-Jan Kindermans, and Quoc V Le. Don't decay the learning rate, increase the batch size. In *International Conference on Learning Representations*, 2018.
- [12] Yang You, Igor Gitman, and Boris Ginsburg. Scaling sgd batch size to 32k for imagenet training. *arXiv preprint arXiv:1708.03888*, 2017.
- [13] Takuya Akiba, Shuji Suzuki, and Keisuke Fukuda. Extremely large minibatch sgd: Training resnet-50 on imagenet in 15 minutes. *arXiv preprint arXiv:1711.04325*, 2017.
- [14] Jorma Rissanen. Modeling by shortest data description. *Automatica*, 14(5):465–471, 1978.
- [15] Pratik Chaudhari, Anna Choromanska, Stefano Soatto, and Yann LeCun. Entropy-sgd: Biasing gradient descent into wide valleys. In *International Conference on Learning Representations*, 2017.
- [16] Stanisław Jastrzebski, Zachary Kenton, Devansh Arpit, Nicolas Ballas, Asja Fischer, Yoshua Bengio, and Amos Storkey. Finding flatter minima with sgd. 2018.
- [17] Chiyuan Zhang, Samy Bengio, Moritz Hardt, Benjamin Recht, and Oriol Vinyals. Understanding deep learning requires rethinking generalization. *arXiv preprint arXiv:1611.03530*, 2016.
- [18] C. S. Wallace and D. M. Boulton. An information measure for classification. *The Computer Journal*, 11(2):185–194, 1968.
- [19] David JC MacKay. A practical bayesian framework for backpropagation networks. *Neural computation*, 4(3):448–472, 1992.
- [20] Samuel L Smith and Quoc V Le. A bayesian perspective on generalization and stochastic gradient descent. In *Proceedings of Second workshop on Bayesian Deep Learning (NIPS 2017)*, 2017.
- [21] Laurent Dinh, Razvan Pascanu, Samy Bengio, and Yoshua Bengio. Sharp minima can generalize for deep nets. In *International Conference on Machine Learning*, pages 1019–1028, 2017.
- [22] Max Welling and Yee W Teh. Bayesian learning via stochastic gradient langevin dynamics. In *Proceedings of the 28th International Conference on Machine Learning (ICML-11)*, pages 681–688, 2011.
- [23] Jia Deng, Wei Dong, Richard Socher, Li-Jia Li, Kai Li, and Li Fei-Fei. Imagenet: A large-scale hierarchical image database. In *Computer Vision and Pattern Recognition, 2009. CVPR 2009. IEEE Conference on*, pages 248–255. IEEE, 2009.
- [24] Alex Krizhevsky. One weird trick for parallelizing convolutional neural networks. *arXiv preprint arXiv:1404.5997*, 2014.

- [25] Léon Bottou. Online learning and stochastic approximations. *On-line learning in neural networks*, 17(9): 142, 1998.
- [26] Ian J Goodfellow, Oriol Vinyals, and Andrew M Saxe. Qualitatively characterizing neural network optimization problems. *arXiv:1412.6544*, 2014.
- [27] Yann LeCun, Léon Bottou, Yoshua Bengio, and Patrick Haffner. Gradient-based learning applied to document recognition. *Proceedings of the IEEE*, 86(11):2278–2324, 1998.
- [28] Alex Krizhevsky and Geoffrey Hinton. Learning multiple layers of features from tiny images. 2009.
- [29] Richard H Byrd, Peihuang Lu, Jorge Nocedal, and Ciyu Zhu. A limited memory algorithm for bound constrained optimization. *SIAM Journal on Scientific Computing*, 16(5):1190–1208, 1995.
- [30] Kaiming He, Xiangyu Zhang, Shaoqing Ren, and Jian Sun. Deep residual learning for image recognition. In *Proceedings of the IEEE Conference on Computer Vision and Pattern Recognition*, pages 770–778, 2016.
- [31] Alex Krizhevsky, Ilya Sutskever, and Geoffrey E. Hinton. Imagenet classification with deep convolutional neural networks. In *Advances in Neural Information Processing Systems*, pages 1097–1105. 2012.
- [32] Hao Li, Zheng Xu, Gavin Taylor, and Tom Goldstein. Visualizing the loss landscape of neural nets. *arXiv preprint arXiv:1712.09913*, 2017.

## Appendix A Proof of Theorem 1 and Theorem 2

### A.0.1 Proof of Theorem 1

*Proof.* As  $\mathcal{D}(\mathbf{w}, a)$  is defined as a box centering at  $\mathbf{w}$  with size  $2a$ , i.e.,

$$\mathcal{D}(\mathbf{w}, a) = \{\mathbf{w}' \in \mathbb{R}^m : |(\mathbf{w}' - \mathbf{w})_i| \leq a, \forall i \in \{1, 2, \dots, m\}\}, \quad (12)$$

then, under *Uniform Perturbation*,

$$\begin{aligned} \bar{C}(\mathbf{w}) &= \mathbf{E} \left\{ \bar{C}(\mathbf{w}; \Theta) \right\} = \mathbf{E} \{ C(\mathbf{w} + \Theta) \} \\ &= \frac{1}{(2a)^m} \int \dots \int_{\mathcal{D}(\mathbf{w}, a)} C(\mathbf{w}') dw'_1 \dots dw'_m \end{aligned} \quad (13)$$

$$\frac{\partial \bar{C}(\mathbf{w})}{\partial w_i} = \frac{1}{(2a)^m} \int \dots \int_{\mathcal{D}(\mathbf{w}_{\setminus i}, a)} \left( C(\mathbf{w}')|_{w'_i=w_i+a} - C(\mathbf{w}')|_{w'_i=w_i-a} \right) dw'_{\setminus i}, \quad (14)$$

where

$$\mathbf{w}_{\setminus i} \triangleq [w_1, \dots, w_{i-1}, w_{i+1}, \dots, w_m]^T \in \mathbb{R}^{m-1} \quad (15)$$

and

$$d\mathbf{w}'_{\setminus i} \triangleq dw'_1 \dots dw'_{i-1} dw'_{i+1} \dots dw'_m. \quad (16)$$

When  $C(\mathbf{w})$  is symmetric about  $\mathbf{w}_f$  in  $\mathcal{D}(\mathbf{w}_f, \tau)$  such that,  $\forall i$ , a cut along  $w_i = (\mathbf{w}_f)_i + a$  and a cut along  $w_i = (\mathbf{w}_f)_i - a$  get the same function in the subspace  $\mathbf{w}_{\setminus i}$ , then  $\nabla \bar{C}(\mathbf{w}_f) = \mathbf{0}$ ; that is, the *Flat Constraint* satisfies with  $\varphi = 0$ .  $\square$

The optimal  $\varphi$  and  $\tau$  are determined by the symmetry of the flat region.  $\varphi$  may be relaxed to a larger value when the symmetry is broken; however, within a flat region, a larger  $\varphi$  may only slightly increase  $C(\mathbf{w}^*)$ .

### A.0.2 Proof of Theorem 2

*Proof.* Suppose  $C_{\varepsilon'}^{(s)}$  is the maximum value near the sharp minimum, i.e.,

$$C_{\varepsilon'}^{(s)} = \max_{\mathcal{D}(\mathbf{w}_s, \varepsilon')} (C(\mathbf{w})), \quad (17)$$

as  $C(\mathbf{w})$  is strictly monotonic in  $\mathcal{D}(\mathbf{w}_s, b)$ , we have,  $\forall \varepsilon' < a < b$ ,

$$\min_{\mathcal{D}(\mathbf{w}_s, a) \setminus \mathcal{D}(\mathbf{w}_s, \varepsilon')} (C(\mathbf{w})) > C_{\varepsilon'}^{(s)}, \quad (18)$$

where  $\mathcal{D}(\mathbf{w}_s, a) \setminus \mathcal{D}(\mathbf{w}_s, \varepsilon')$  is a *Set Difference*, notating a domain within  $\mathcal{D}(\mathbf{w}_s, a)$  but outside of  $\mathcal{D}(\mathbf{w}_s, \varepsilon')$ .

Then, follow the proof of Theorem 1, we have

$$\begin{aligned} \min_{\mathcal{D}(\mathbf{w}_s, \varepsilon) | \varepsilon < b} (\bar{C}(\mathbf{w})) &= \frac{1}{(2a)^m} \int \dots \int_{\mathcal{D}(\mathbf{w}_s, a)} C(\mathbf{w}') dw'_1 \dots dw'_m \\ &\geq \frac{1}{(2a)^m} \cdot \left( (2a)^m C_{\varepsilon'}^{(s)} - (2\varepsilon')^m (C_{\varepsilon'}^{(s)} - C(\mathbf{w}_s)) \right) \\ &= \left( 1 - \left( \frac{\varepsilon'}{a} \right)^m \right) C_{\varepsilon'}^{(s)} + \left( \frac{\varepsilon'}{a} \right)^m \cdot C(\mathbf{w}_s). \end{aligned} \quad (19)$$

Because of

$$\lim_{m \rightarrow \infty} \left( \left( 1 - \left( \frac{\varepsilon'}{a} \right)^m \right) C_{\varepsilon'}^{(s)} + \left( \frac{\varepsilon'}{a} \right)^m \cdot C(\mathbf{w}_s) \right) = C_{\varepsilon'}^{(s)}, \quad (20)$$

in high dimensional models (like deep neural networks), we can find  $\varepsilon \rightarrow \varepsilon'^- \rightarrow a^-$  (left limit) to satisfy

$$\min_{\mathcal{D}(\mathbf{w}_s, \varepsilon)} (\bar{C}(\mathbf{w})) > C_{\varepsilon'}^{(s)} \triangleq \max_{\mathcal{D}(\mathbf{w}_s, \varepsilon)} (C(\mathbf{w})). \quad (21)$$

In the flat region,

$$\begin{aligned} \min_{\mathcal{D}(\mathbf{w}_f, \tau)} (\bar{C}(\mathbf{w})) &= \frac{1}{(2a)^m} \int \dots \int_{\mathcal{D}(\mathbf{w}_f, a)} C(\mathbf{w}') dw'_1 \dots dw'_m \\ &< \frac{1}{(2a)^m} \cdot \left( (2a)^m \cdot \max_{\mathcal{D}(\mathbf{w}_f, a)} (C(\mathbf{w})) \right) \\ &= \max_{\mathcal{D}(\mathbf{w}_f, a)} (C(\mathbf{w})) \triangleq C_a^{(f)} \end{aligned} \quad (22)$$

Assuming  $C(\mathbf{w}_s) \approx C(\mathbf{w}_f)$ , as  $a$  grows,  $C_\varepsilon^{(s)}|_{\varepsilon \rightarrow a^-}$  increases fast in the sharp region while  $C_a^{(f)}$  increases slowly in the flat region; therefore,  $\exists a$  such that

$$C_\varepsilon^{(s)} > C_a^{(f)}. \quad (23)$$

According to Inequality (21)(22)(23),

$$\min_{\mathcal{D}(\mathbf{w}_s, \varepsilon)} (\bar{C}(\mathbf{w})) > \max_{\mathcal{D}(\mathbf{w}_s, \varepsilon)} (C(\mathbf{w})) > \max_{\mathcal{D}(\mathbf{w}_f, a)} (C(\mathbf{w})) > \min_{\mathcal{D}(\mathbf{w}_f, \tau)} (\bar{C}(\mathbf{w})) \quad (24)$$

which satisfies the *Sharp Constraint*. □

## Appendix B Sensitivity Analyses

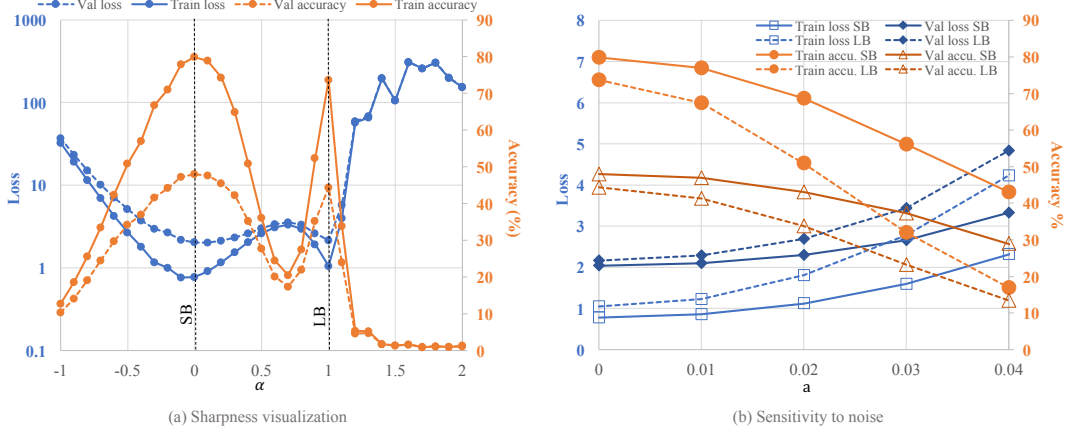


Figure 7: Notation: “SB”: Small Batch (256); “LB”: Large Batch (5000); “accu.”: accuracy. (a) loss and accuracy vs.  $\alpha$ , which controls  $w$  along the direction from SB minimum ( $w_f$ ) to LB minimum ( $w_s$ ); (b) loss and accuracy under influence of different strengths of noise. Dataset: CIFAR-100. Network:  $C_3$  in [2] implemented by [9]. The optimizer is Adam with 0.001 initial learning rate.

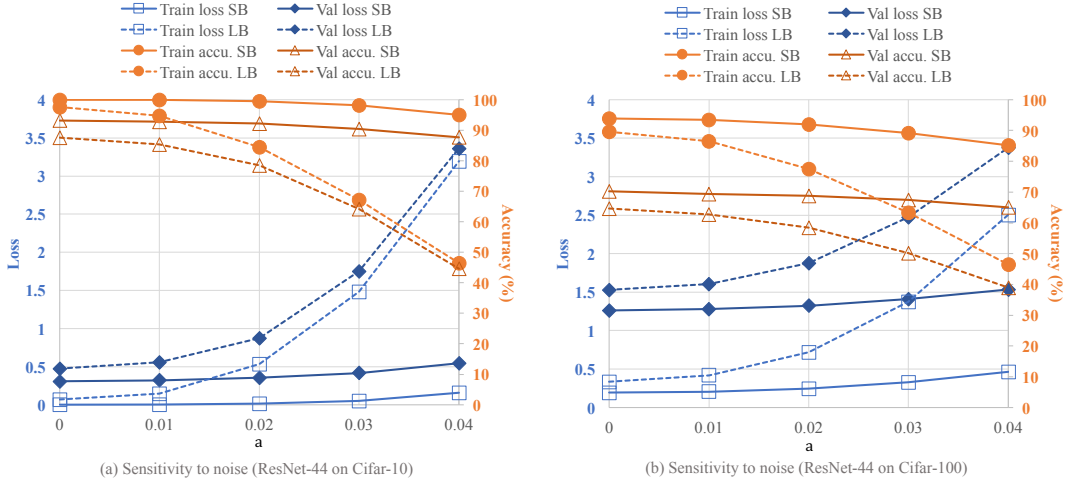


Figure 8: Loss and accuracy of ResNet-44 under influence of different strengths of noise on (a) CIFAR-10 and (b) CIFAR-100 implemented by [9]. The optimizer is SGD with momentum 0.9. Notation: “SB”: Small Batch (128); “LB”: Large Batch (2048 for CIFAR-10 and 1024 for CIFAR-100); “accu.”: accuracy.

## Appendix C Sharpness Visualization

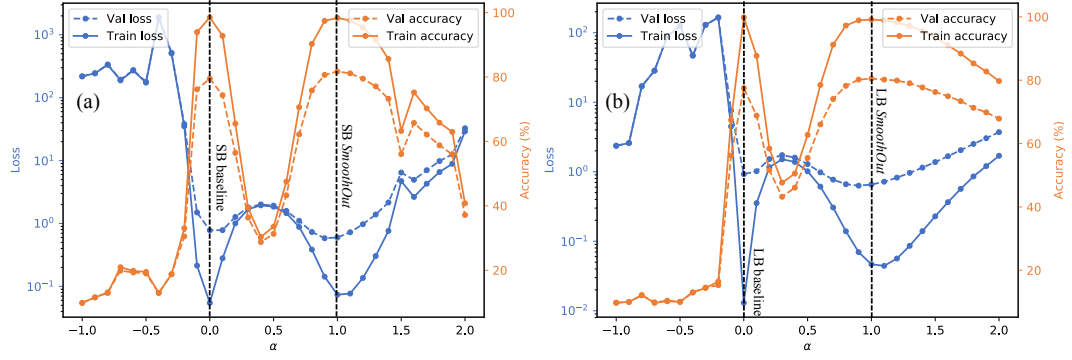


Figure 9: Sharpness of baseline and *SmoothOut* in (a) “SB” training and (b) “LB” training of  $C_1$ .

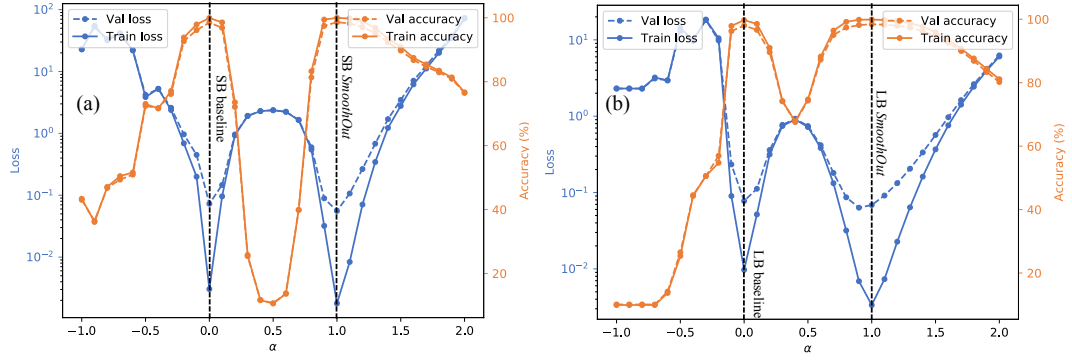


Figure 10: Sharpness of baseline and *SmoothOut* in (a) “SB” training and (b) “LB” training of  $F_1$ .